

Faradaic Efficiencies for Methanol Oxidation in Proton-Exchange Membrane Electrolysis and Fuel Cells with Various Anode Catalysts

Rakan M. Altarawneh

Department of Chemistry, Faculty of Science, Mu'tah University, Al-Karak, Jordan
Corresponding author. Tel.: 00962776193935
E-mail: rma766@mutah.edu.jo

Received: 29 March 2019 / Accepted: 6 June 2019 / Published: 30 June 2019

The energy efficiency of a direct methanol fuel cell (DMFC) is dependent on the cell voltage, crossover of oxygen and/or methanol through the polymer electrolyte membrane, and stoichiometry of the methanol oxidation reaction (i.e., the average number of electrons transferred per methanol molecule (n_{av})). The stoichiometry is determined by the product distribution (carbon dioxide: formic acid: formaldehyde) and the amount of methanol consumed. The influence of crossover is investigated by using air and N₂ at the cathode. Accurate determination of n_{av} requires analysis of the methanol and products from both the anode and cathode and quantitative determination of the consumption of methanol. In this work, n_{av} values obtained from the analysis of the cell exhausts by proton NMR and infrared spectrometry are compared with values obtained from a simple electrochemical method based on the dependence of the current on the flow rate of the methanol solution. The methodology presented here provides a comprehensive evaluation of methanol oxidation, along with a full determination of the methanol consumption and hence the fuel efficiency of the cell. The methods are suitable for rapid evaluation of catalysts in fuel cell hardware with low-cost online sensors for determination of product distributions.

Keywords: direct methanol fuel cell; methanol electrolysis cell; crossover; product distribution; flow rate; stoichiometry; efficiency

1. INTRODUCTION

Methanol is an attractive fuel for direct alcohol fuel cells (DAFCs). It possesses some advantages, such as simple handling and storage, a suitable high energy density, and the low cost of methanol. [1–7] The direct methanol fuel cell (DMFC) is an efficient device that converts the chemical energy of methanol into electricity. Combining these highly efficient fuel cell systems with the renewable aspect

of methanol has the potential to create a nearly carbon-neutral device. It is considered an attractive power source with much potential for electronic devices and vehicles. [8–12]

However, the commercialization of DMFCs has been hindered by some crucial issues. The most important is the low power density caused by the incomplete oxidation of methanol to formic acid and formaldehyde, as well as crossover of methanol. [8, 13–15] Therefore, modification of commercial catalysts and preparation of new catalysts are required to increase cell efficiencies by facilitating the complete oxidation of methanol, and methods are required for their comprehensive evaluation under fuel cell conditions. [5, 13–20] The methodologies reported here can provide information on the efficiency and product distribution of the oxidation of methanol in a DMFC or methanol electrolysis cell. The efficiencies of these cells are dependent on the cell voltage, methanol crossover, and stoichiometry of the methanol oxidation reaction. The stoichiometry, efficiency, and product distribution of methanol in fuel cell hardware were determined at 50 °C for various anodes prepared with commercial platinum (Pt) black, platinum-ruthenium (PtRu) black, and platinum tin (PtSn) black catalysts. A non-dispersive infrared CO₂ monitor was used to measure CO₂, while the amounts of formic acid and formaldehyde produced and methanol consumed were determined by proton NMR spectroscopy. [20–21]

2. EXPERIMENTAL

2.1 The cell

Commercial 5 cm² active area fuel cell hardware (Fuel Cell Technology Inc.) was operated in two different modes, as shown in Fig. 1, with a Pt black cathode and various anodes. These operating modes are fuel cell mode (direct methanol fuel cell mode, DMFC) and electrolysis mode (pseudo-half-cell mode (phc mode) or anode polarization mode), which have been described previously. [21–26] The gas at the cathode side is only the difference between those two modes. In both modes, aqueous methanol (Commercial Alcoholic Inc.) solution (0.10 M in water) was supplied to the anode at various flow rates (0.5, 0.2, 0.09, 0.05, 0.02, and 0.01 ml min⁻¹) with a syringe pump. Air (or oxygen) or N₂ was passed over the cathode at ca. 30 cm³ min⁻¹ with respect to the mode employed (Fig. 1). In pseudo-half-cell mode, N₂ is used to avoid interference from oxygen, and the cathode acts as a dynamic hydrogen electrode (DHE). [20–21] Membrane and electrode assemblies (MEAs) were prepared as previously described [23–26] by pressing a 5 cm² anode and 5 cm² cathode onto a Nafion™115 membrane (acidic polymer electrolyte) in the cell. Anodes consisted of 4 mg cm⁻² Pt black, PtRu black, and PtSn black on Toray™ (TGP-H-090) carbon fibre paper, while 4 mg cm⁻² Pt black on TGP-H-090 was used as a cathode. A Hokuto Denko HA-301 potentiostat was used to perform the electrochemical measurements at 50 °C at constant cell potentials under steady-state conditions.

2.2 Methanol and product analysis

The schematic diagrams of the product collection apparatus are shown in Fig. 1. At each potential, the cell was operated at various flow rates of methanol. The liquid and gas from both the anode and cathode exhausts were combined at each flow rate and collected in a trap cooled with a mixture of

ice and dry ice before analysis. The gas (air or nitrogen) leaving the trap was passed through a commercial non-dispersive infrared CO₂ monitor (Telaire 7001) to measure the CO₂ in real time. Methanol, formic acid, and formaldehyde remaining in the trap were measured by using ¹H NMR spectroscopy. [21, 23–26]

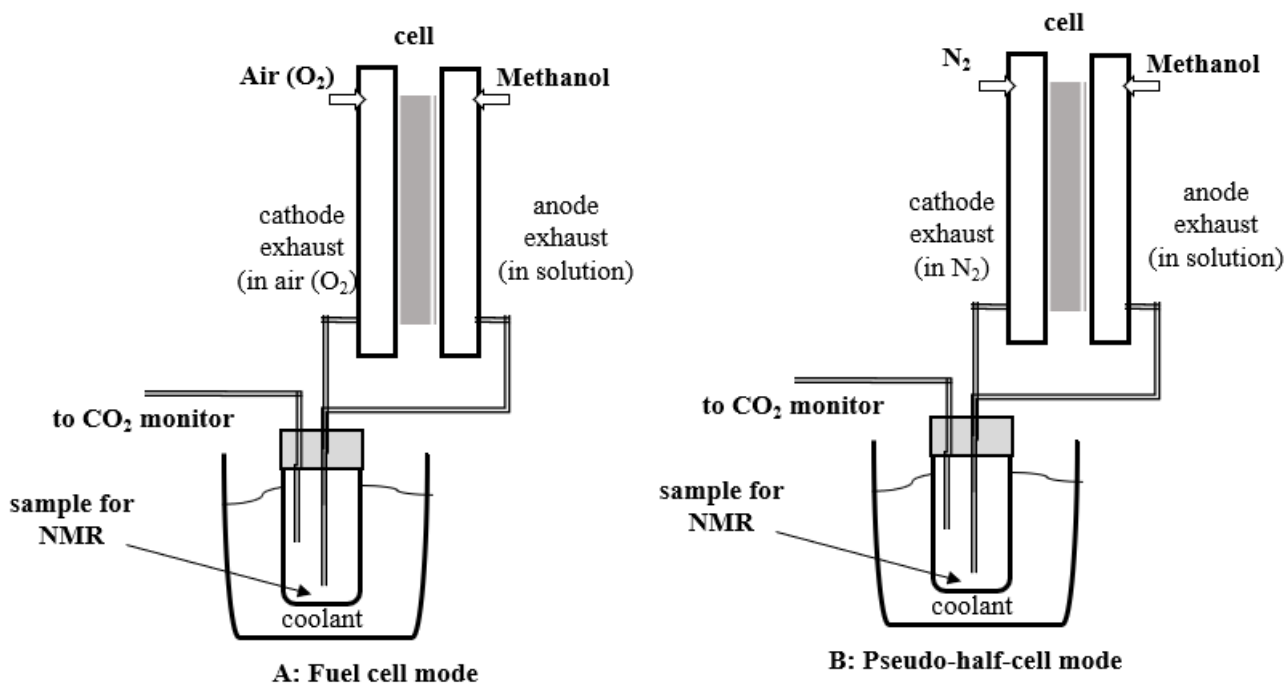


Figure 1. Schematic diagrams of the product collection systems employed in this work.

3. RESULTS AND DISCUSSION

3.1 Polarization curves

To investigate the effect of Ru addition and the influence of using air (or O₂) at the cathode on the activity of the Pt anode catalyst in a direct methanol fuel cell (DMFC), the cell was first operated in fuel cell mode (Fig. 1A) with Pt and PtRu anode catalysts. Fig. 2 compares polarization curves for methanol oxidation (0.1 M aqueous solution) at the Pt black and PtRu black anodes with air at the cathode. As reported in many previous studies, [27, 28] the current was much higher at all potentials when the PtRu black catalyst was used as an anode catalyst than when Pt black was used as an anode catalyst, indicating that the PtRu anode catalyst has higher activity than the Pt anode catalyst for methanol oxidation. This result can be explained as in many previous reports as follows: the production of poisoning species (CO_{ad} and OH_{ad} at low and at high current regions, respectively) causes a decrease in selectivity and catalytic activity by inhibiting the adsorption and further oxidation of methanol. [10, 29] Generally, in this operating mode, the activity of an anode is limited at high potentials by dissociative adsorption of water that is required for CO tolerance. At low potentials, the activity of those anodes is limited by mass transport (methanol diffusion) through the carbon fibre paper backing layer where the current levelled off (limiting current region), which happens when the methanol concentration is low.

[20] The enhancement in the activity of the PtRu anode at high potentials (or at low potentials with N₂ at the cathode; see below) is usually ascribed to a bifunctional mechanism (OH_{ad} formation). [10, 18, 28, 30]

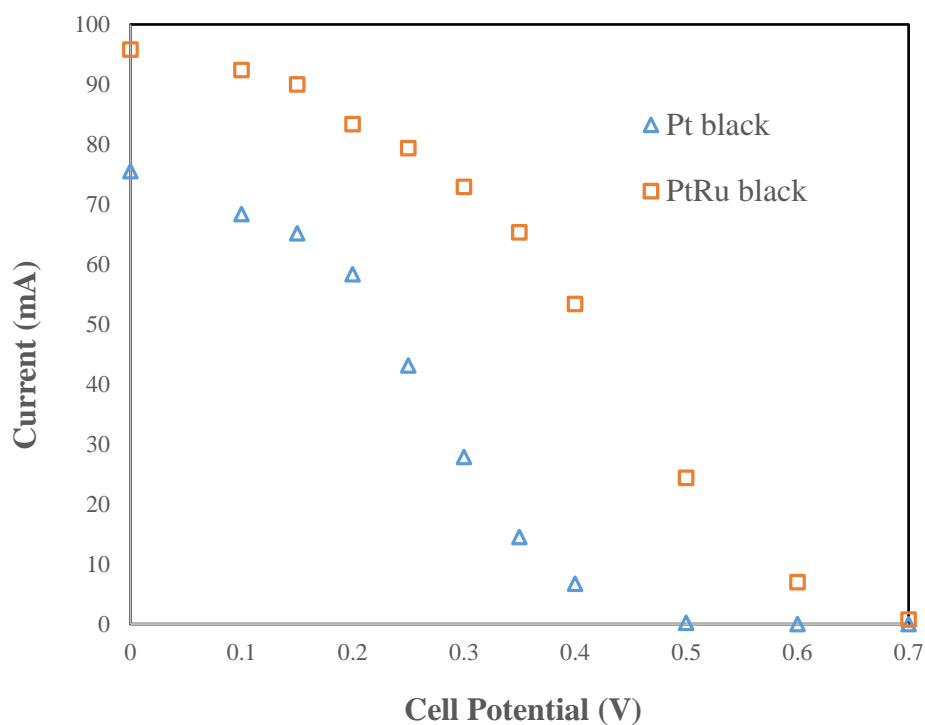


Figure 2. Fuel cell polarization curves for methanol oxidation (0.100 M aqueous methanol solution at a flow rate of 0.5 mL min⁻¹) at Pt black and PtRu black anodes at 50 °C.

Fig. 3 shows the polarization curves for the oxidation of 0.1 M methanol at the Pt black, PtRu black and PtSn black anodes in pseudo-half-cell mode (Fig. 1B). It is clear from this figure that among the three anodes, the PtRu anode provides the highest activity at all potentials, while the Pt anode has the lowest activity for methanol oxidation. The current at the PtSn black anode was intermediate between those at the PtRu and Pt black anodes. [31–32] The higher activity of the PtRu anode at low potentials is attributed to the bifunctional mechanism, while it is limited at high potential by mass transport. [27–28]

Comparing the results in Fig. 2 shows that the PtRu and Pt anodes have the same behaviour (almost the same activity) in the limiting current region in both modes, which means that using air or N₂ at the cathode did not significantly affect the activity of the electrode in this current region. In the low-current region where the crossover is significant, the activities of those anodes were higher when using N₂ instead of O₂ at the cathode. Generally, the amount of oxygen crossover from the cathode side of a fuel cell to the anode increases as the current density decreases. [20] Consequently, oxygen can improve CO tolerance by oxidizing CO and thus increases the adsorption and further oxidation of methanol, resulting in higher activity. [33–36] However, the data in Fig. 2 and 3 are opposed to this explanation, where the activity should be higher in the low-current region when using O₂. This finding may be explained as follows: since the chemical reaction does not produce a current in the external circuit, the lower anode activity in the low-current region in a fuel cell can be attributed to the facile chemical

reaction between oxygen and methanol in the anode due to crossover. This process leads to an increase in the undesirable utilization of methanol (chemical oxidation) in the anode, resulting in lower activity.

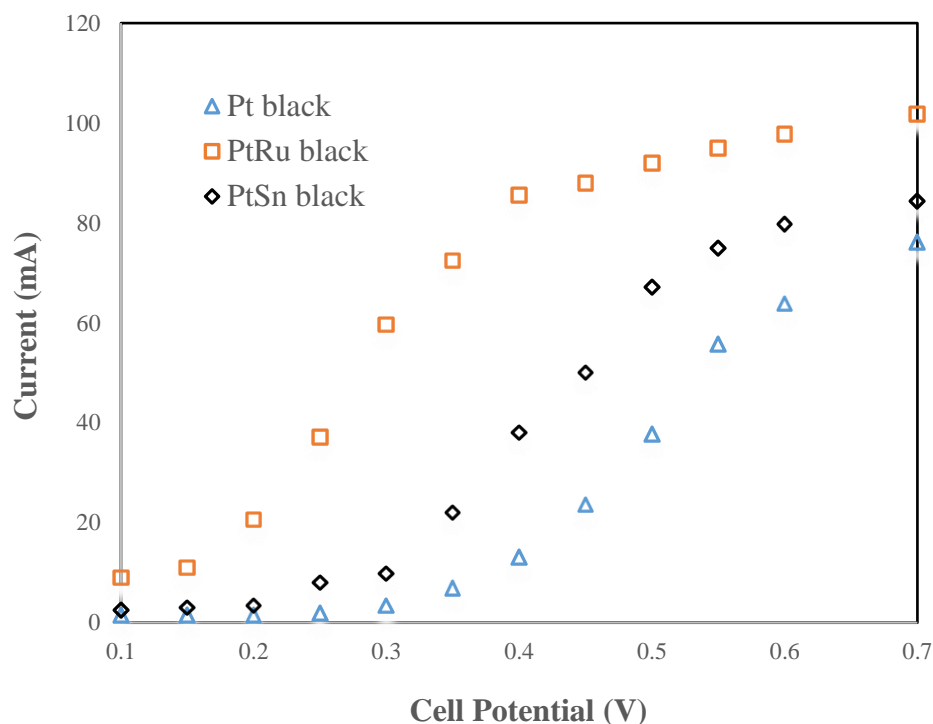


Figure 3. Polarization curves for methanol oxidation (0.100 M aqueous methanol solution at a flow rate of 0.5 mL min^{-1}) at different anode catalysts (Pt black, PtRu black, and PtSn black) in pseudo-half-cell mode (Fig. 1B) at $50 \text{ }^\circ\text{C}$.

3.2 Product distributions

Based on my knowledge, a number of research groups have determined CO_2 yields from DMFCs or under fuel cell operating conditions. Additionally, most of the studies on alcohol fuel cells have been performed at room temperature in a liquid electrolyte, and these studies have only been analysed based on the electrical performance, as in the last section, for example (polarization curves). By contrast, commercial fuel cells are operated at relatively elevated temperatures (ca. $70 \text{ }^\circ\text{C}$ - $120 \text{ }^\circ\text{C}$) using a solid electrolyte. [37–41] Therefore, the cell in this study was run at $50 \text{ }^\circ\text{C}$ using a polymer membrane as an electrolyte, and for the next step, the cell will be run at $80 \text{ }^\circ\text{C}$. Different procedures can be used to establish a correlation between operating conditions and fuel crossover and then overall efficiency. [21] Ultimately, these results can help understand and develop an efficient fuel cell system after taking into account the durability of membranes and catalysts at those elevated temperatures and the effect of crossover on the overall efficiency. [42]

Fig. 4 shows the faradaic CO_2 yields for methanol oxidation at various anodes at different flow rates in both modes. Since the main product is carbon dioxide with yields higher than 80% and the measured formaldehyde is known to be inaccurate (estimated by mass balance), the results for formic acid and formaldehyde are not shown here. The faradaic yields of CO_2 demonstrate the effects of using air or N_2 at the cathode. When the cell is operated in fuel cell mode (DMFC), methanol is electrochemically and chemically oxidized at both the anode and cathode, where the chemical oxidation

is due to the crossover of oxygen and/or methanol through the membrane (from the cathode to the anode, or vice versa). Errors due to the crossover of oxygen and/or methanol are significant at all flow rates of methanol solution and even at various potentials for the same electrode. The crossover leads to a chemical reaction between O_2 and methanol at both the anode and cathode, resulting in higher CO_2 yields and then inaccurately calculated n_{av} values. Although this chemical reaction generates CO_2 , formic acid, and formaldehyde, it does not produce a current in the external circuit.

It is clearly observed from Fig. 4A that the CO_2 yields were higher when the cell was operated with air at the cathode. Using oxygen at the cathode leads to overestimation of the products and methanol consumed due to the chemical reaction, providing inaccurate results. Fig. 4B shows more accurate CO_2 yields, which provide accurate n_{av} values when the cell was operating in anode polarization mode with N_2 at the cathode.

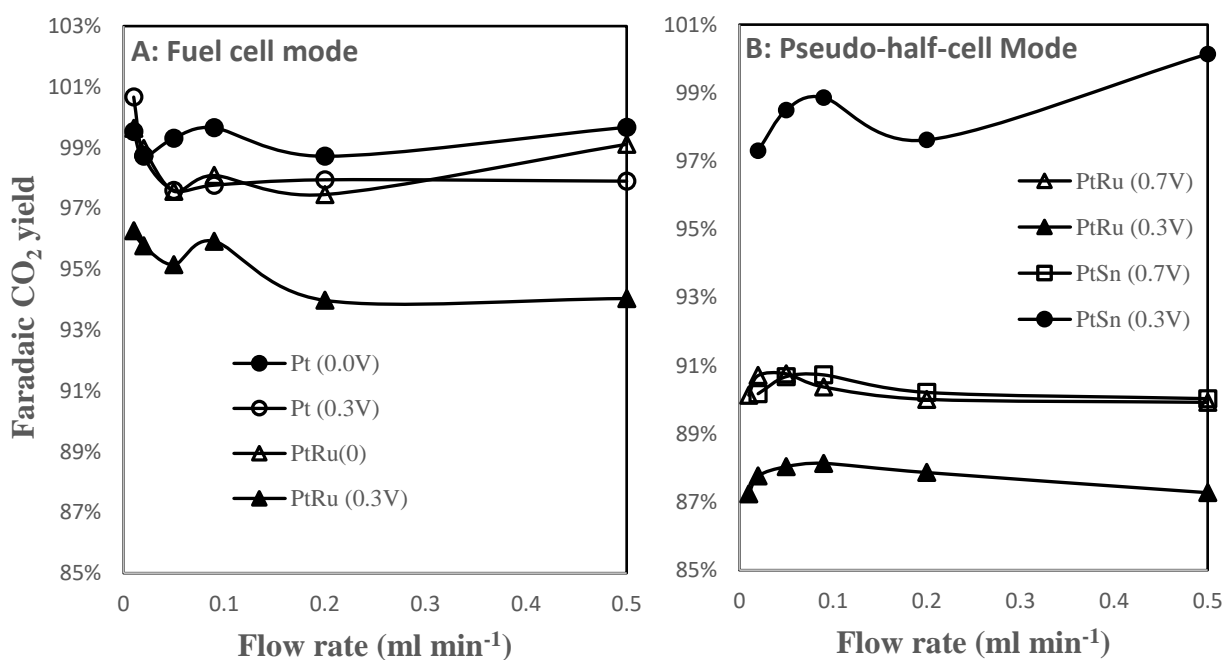


Figure 4. Faradaic yields of CO_2 for the anode and cathode exhausts vs. flow rates of methanol (0.10 M) at 50 °C of a cell operating in (A) fuel cell mode and (B) pseudo-half-cell mode at a flow rate of 0.2 mL min⁻¹.

Neither et al. [43] studied the effect of temperature on CO oxidation from polymer electrolyte fuel cells using differential electrochemical mass spectrometry (DEMS). They reported that increasing the operating temperature led to enhanced CO tolerance. James and Pickup [44] have shown the effect of using oxygen at the cathode on the product yields in direct ethanol fuel cells (DEFCs). They reported that using oxygen leads to an overestimation of product yields due to crossover. Wang et al. [45] used DEMS to determine the product distribution at various catalysts in a cell with a liquid electrolyte at room temperature. It was found that modification of Pt with Ru increased the activity and selectivity (CO_2 formation) at low potentials.

Generally, different procedures can be used to investigate the crossover in such cells, such as analysing the fuel itself and its products in the polymer membrane or in the cathode exhaust (in addition

to anode exhaust), as described in previous reports for ethanol. [46–49] In this study, to demonstrate the dependence of crossover on the cell potentials, the amount of methanol consumed was measured at two different potentials when the cell was operated in fuel cell mode and pseudo-half-cell mode. Generally, the consumption of methanol should be higher in the high-current region (herein, at 0.7 V in pseudo-half-cell mode and 0.0 V in fuel cell mode) than in the low-current region. In addition, in previous studies, it was found that the amount of crossover of O₂ and/or methanol is significantly higher in the low-current region. [20] Fig. 5 shows the amount of methanol consumed at the PtRu black anode at two different potentials when using air and N₂ at the cathode. Measurements at 0.0 and 0.3 V at the PtRu anode in fuel cell mode revealed that almost the same amounts of methanol were consumed, showing that there was a facile crossover of O₂ and/or methanol through the membrane at 0.3 V, resulting in higher yields of the chemical reaction. In contrast, the crossover has less effect on the amount of methanol consumed and product distribution in the absence of O₂ when using N₂ at the cathode in pseudo-half-cell mode (there is no chemical reaction). Consequently, different amounts of methanol consumption were measured at 0.7 and 0.3 V at the PtRu anode in this mode, as shown in Fig. 5.

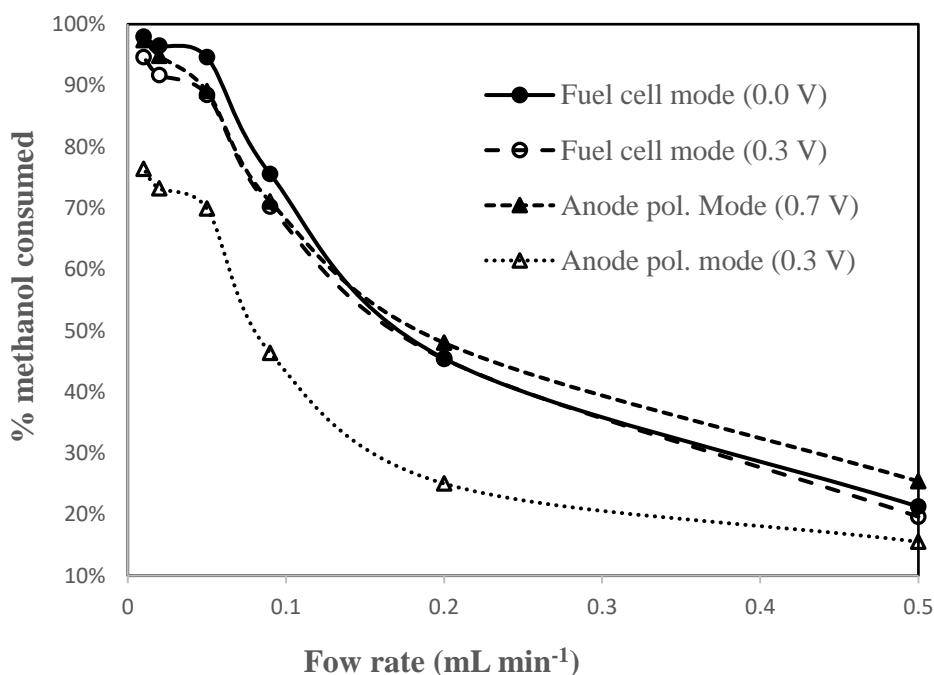


Figure 5. Percentage of methanol consumed vs. flow rate of methanol (0.01, 0.02, 0.5, 0.9, 0.2, and 0.5 mL min⁻¹) for the oxidation of 0.1 M methanol at the PtRu black anode in fuel cell mode and pseudo-half-cell mode at 50 °C.

3.3 Stoichiometry and faradaic efficiency

The n_{av} values obtained in this work using different methods are presented in Table 1. The procedure for determining n_{av} by these methods has been previously described. [23–26] These methods are an electrochemical method based on the dependence of the current (i) on the flow rate (u) of the

methanol solution and product distribution methods based on the amount of methanol consumed, faradaic yield, and chemical yield. Since the concentration of methanol through the anode flow field decreases with decreasing methanol flow rate, [20] various flow rates of methanol solution were used to study the variation in stoichiometry with methanol concentration. It is clear from Table 1 that there are no significant changes in n_{av} with concentration. It should be noted that n_{av} values obtained from each method represent averages over the range of flow rates employed.

It can be seen that there is good agreement between the values calculated based on those methods with N₂ at the cathode and that the small discrepancies can be attributed to a systematic error. However, using O₂ at the cathode significantly overestimated the n_{av} values calculated from faradaic yields, which can be attributed to the crossover of O₂ and/or methanol. Comparing the results for PtRu black in fuel cell mode and pseudo-half-cell mode reveals that the n_{av} values were much higher with O₂ at the cathode. The higher n_{av} values in fuel cell mode can be attributed to the chemical reaction, as described earlier. Interestingly, the n_{av} was ca. 6.0 at the PtSn anode at 0.3 V, which is consistent with the higher yields of CO₂ shown in Fig. 4B. However, since the activities of the PtSn anode in Fig. 3 were lower than those at the PtRu anode and n_{av} (Table 1) was higher for the PtSn anode than the PtRu anode at 0.3 V, the polarization curve cannot clearly demonstrate the synergistic effect of modifying Pt with other metals such as Ru and Sn. [49–51]

The average n_{av} values were used to determine the faradaic efficiency ($\epsilon_f = n_{av}/6$) for each anode under certain conditions, as shown in Table 1. The faradaic efficiencies show that the PtSn anode at 0.3 V has the highest selectivity for the complete oxidation of methanol to CO₂, while its selectivity decreases significantly at 0.7 V. In contrast, the selectivity at the PtRu anode in fuel cell mode was much higher at 0.0 V than at 0.3 V. At the Pt and PtRu (in Pseudo-half-cell mode) anodes, the selectivity was not changed significantly at high or low potentials.

Table 1. Summary of n_{av} values obtained in this work and faradaic efficiencies (ϵ_f) for methanol oxidation. Averages and standard deviations for five consecutive experiments at different flow rates are presented.

Anode catalyst	Mode	Potential/V	n_{av}					
			i vs. u	Methanol consumed	faradaic yields	chemical yields	Average n_{av}	ϵ_f
Pt black	Fuel cell	0.0	5.24	5.73±0.07	5.95±0.06	5.81±0.04	5.43±0.31	95%
Pt black	Fuel cell	0.3	5.17	5.62±0.24	5.85±0.15	5.69±0.13	5.58±0.29	93%
PtRu black	Fuel cell	0.0	5.97	5.65±0.06	5.84±0.10	5.71±0.04	5.79±0.14	97%
PtRu black	Fuel cell	0.3	5.05	4.85±0.10	5.49±0.10	5.09±0.05	5.12±0.27	85%
PtRu black	phc mode*	0.7	5.05	4.95±0.13	5.04±0.02	4.99±0.08	5.01±0.05	83%
PtRu black	phc mode*	0.3	4.65	5.11±0.67	4.83±0.02	4.99±0.39	4.90±0.20	82%
PtSn black	phc mode*	0.7	4.34	4.68±0.33	5.06±0.02	4.83±0.19	4.73±0.30	79%
PtSn black	phc mode*	0.3	6.00	5.94±0.10	5.85±0.14	5.90±0.08	5.92±0.06	99%

- phc mode:- Pseudo-half-cell mode

4. CONCLUSIONS

The electrochemical method yields results that are consistent with those based on the consumption of methanol and product analysis, which can be used for rapid routine determination of n_{av} and hence the fuel efficiency of the cell. Using O_2 at the cathode will not significantly affect the anode activities in the limiting current region but does change the product distribution and thus the faradaic efficiency. The anode activity in the low-current region increased with nitrogen at the cathode due to the absence of the chemical reaction. In pseudo-half-cell mode, errors due to crossover are smaller when using N_2 instead of O_2 at the cathode. However, the enhancement in the activities of Pt was much higher at all potentials after modification with Ru, while Sn increased the Pt activities at intermediate potentials. The best selectivity was observed for the PtSn anode at 0.3 V.

ACKNOWLEDGMENTS

I would like to dedicate this article to Professor Peter Pickup, my Ph.D. supervisor, whose friendship and advice have always been a source of encouragement.

References

1. S. K. Kamarudin, N. S. Shamsul, J. A. Ghani, S.K. Chia, H.S. Liew, and A.S. Samsudin. *Bioresour. Technol.*, 129 (2013) 463.
2. R. N. Singh, R. Awasthi, and C. S. Sharma. *Int. J. Electrochem. Sci.*, 9 (2014) 5607.
3. B. C. Ong, S. K. Kamarudin, and S. Basri. *Int. J. Hydrogen Energy* 42 (2017) 10142.
4. P. Iotov and S. Kalcheva. *J. Chem. techn. metall.*, 48 (2013) 80.
5. T. Huang, S. Mao, G. Zhou, Z. Zhang, Z. Wen, X. Huang, S. Cib, and J. Chen. *Royal Soc. Chem.*, 7 (2015) 1301.
6. R. A. Mirzaie, and A. Eshghi. *J. Surf. Eng.*, 30 (2014) 263.
7. L. Gong, Z. Yang, K. Li, W. Xing, and C. Liu. *J. Energy Chem.*, 27 (2018) 1618.
8. S. Balasubramanian, B. Lakshmanan, C. E. Hetzke, V. A. Sethuraman, and J. W. Weidner. *Electrochim. Acta.*, 58 (2011) 723.
9. N. Akiya and P. E. Savage. *AIChE J.*, 41 (2014) 19.
10. J. J. Baschuk and X. Li. *Int. J. Energy Res.*, 713 (2001) 695.
11. J. N. Tiwari, R. N. Tiwari, G. Singh, and K. S. Kim. *Nano Energy*, 2 (2013) 553.
12. F. Zenith, Y. Na and U. Krewer. *IFAC-PapersOnLine*, 48 (2015) 722.
13. H. Wang, T. Loffler, and H. Baltruschat. *J. Appl. Electrochem.*, 31 (2001) 759.
14. S. Celik, and M. D. Mat. *Int. J. Hydrogen Energy*, 35 (2010) 2151.
15. M. Chen, M. Wang, Z. Yang, X. Ding, and X. Wang. *Electrochim. Acta.*, 282 (2018) 702.
16. A. M. Prasad, C. Santhosh, and A. N. Grace. *Appl Nanosci.*, 2 (2012) 457.
17. M. A. Abdelkareem, N. Morohashi, and N. Nakagawa. *J. Power Sources*. 172 (2007) 659.
18. L. Li and Y. Xing. *Energies*. (2009) 789.
19. S. Basri, S. K. Kamarudin, W. R. W. Daud, Z. Yaakob, and A. A. H. Kadhum. *Scientific World J.*, Article ID 547604, (2014).
20. P. Majidi, R. M. Altarawneh, N. D. W. Ryan, and P. G. Pickup. *Electrochim. Acta* 199 (2016) 210.
21. R. M. Altarawneh, P. Majidi and P. G. Pickup. *J. Power Sources*. 351 (2017) 106.
22. M. Stähler, and A. Burdzik. *J. Power Sources*. 262 (2014) 147.
23. R. M. Altarawneh, T. M. Brueckner, B. Chen, and P. G. Pickup. *J. Power Sources* 400 (2018) 369.
24. R. M. Altarawneh and P. G. Pickup. *J. Electrochem. Soci.*, 165, (2018).
25. R. M. Altarawneh and P. G. Pickup. *J. Electrochem. Soc.* 164 (2017) F861.

26. R. M. Altarawneh and P. G. Pickup. *J. Power Sources* 366 (2017) 27.
27. S. Y. Huang, C. T. Yeh. *J. Power Sources*. 195 (2010) 2638.
28. O. Sahin, H. Kivrak. *Int J Hydrogen Energy*. 38 (2013) 901.
29. G. Liu, X. Li, M. Wang, M. Wang, J. Y. Kim, J. Y. Woo, X. Wang, and J. K. Lee Liu. *Energy Convers. Manag.*, 126 (2016) 697.
30. F. Zenith, Y. Na and U. Krewer. *Energies*, 8 (2015) 10409.
31. A. O. Neto, R. R. Dias, M. M. Tusi, M. Linardi, SE. V. pinace. *J Power Sources*. 166 (2007) 87.
32. M. Amani, M. Kazemeini, M. Hamedanian, H. Pahlavanzadeh, H. Gharibi. *Mater Res Bull*. 68 (2015) 166.
33. V. K. Puthiyapura, W. F. Lin, A. E. Russell, D. J. L. Brett, and C. Hardacre. *Top. Catal*. 61 (2018) 240.
34. A. Ostroverkh and R. Fiala. *Renewable Energy*. 138 (2019) 409.
35. J. Polá, V. Johánek, A. Ostroverkh, and K. Ma. *Materials Chemistry and Physics*. 228 (2019) 147.
36. A. Tomita, J. Nakajima, and T. Hibino. *Angew. Chem. Int.*, 47 (2008) 1462.
37. Y. Sik, *et al. Appl. Surf. Sci.*, 290 (2014) 246.
38. M. Wang, M. Chen, Z. Yang, Y. Wang, Y. Wang, G. Liu, J. K. Lee, and X. Wang. *Energy Convers. Manag.*, 168 (2018) 270.
39. G. Liu, X. Li, M. Wang, M. Wang, J. Y. Kim, J. Y. Woo, X. Wang, and J. K. Lee. *Energy Convers. Manag.*, 138 (2017) 54.
40. M. A. Abdelkareem, A. Allagui, E. T. Sayed, M. El Haj Assad, Z. Said, and K. Elsaid. *Renew. Energy*, 131 (2019) 563.
41. A. S. Aricò, P. Cretì, P. L. Antonucci, and V. Antonucci. *Electrochem. Solid-State Lett.*, 1 (1998) 66.
42. J. Liu, C. Liu, L. Zhao, and Z. Wang. *J. Nanomaterials*, (2015).
43. C. Niether, M.S. Rau, C. Cremers, D.J. Jones, K. Pinkwart, J. Tübke. *J Electroanal. Chem.*, 747 (2015) 97
44. D. D. James, P. G. Pickup. *Electrochim. Acta*, 55 (2010) 3824.
45. H. Wang, C. Wingender, H. Baltruschat, M. Lopez, M. T. Reetz. *J Electroanal. Chem.*, 509 (2001) 163.
46. Y. Paik, S. Kim, and O. H. Han. *Electrochem. Communic.*, 11 (2009) 302.
47. J. B. Day, P. A. Vuissoz, E. Oldfield, Andrzej Wieckowski, and J. P. Ansermet. *J. Am. Chem. Soc.*, 118 (1996) 13046.
48. B. C. Ong, S. K. Kamarudin, S. Basri. *Int. J. Hydrogen Energy*, 42 (2017) 10142.
49. T. Jurzinsky, P. Kurzahls, C. Cremers. *J. Power Sources*, 389 (2018) 61.
50. S.S. Mahapatra, A. Dutta, J. Datta. *Int. J. Hydrogen Energy*, 36 (2011) 14873.
51. C. Lamy, T. Jaubert, S. Baranton, C. Coutanceau. *J. Power Sources*, 245 (2014) 927.